Optimization of Pulsed Current Electrochemical Micro Machining of MONEL 400 Alloy in NaNO₃ Electrolyte

L. Gokulanathan[*], *A.Jegan*

Department of Mechanical Engineering, Sona College of Technology, Salem, Tamil Nadu, India - 636005.
[*]E-mail: lgokulanathan@gmail.com

Components having micro-holes find wide application in fields like aircraft, automobile, healthcare, power circuit boards and ink jet printing nozzles. Monel 400 alloy which is a mixture of nickel and copper is the prime material used for such components. Experiments were conducted by supplying pulsed atmospheric air to the electrolyte with a view to effectively remove the residual machined material. Micro holes were machined using (ECMM) and a single electrolyte. The machining factors namely the percentage of the electrolyte, applied voltage, duty cycle and frequency had been taken as dominant factors. Their optimal combination was arrived using standard optimization techniques, such as, Technique of Order Preference Similarity to the Ideal Solution (TOPSIS), VlseKriterijumskaOptimizacijaKompromisnoResenje (VIKOR) and Complex Proportional Assessment (COPRAS), using material removal rate (MRR) and overcut as response metrics. All the three methods indicated the same optimal parameter combinations. All three methods exposes the same optimal parameter combinations that 28 g/l, 13 V, 75 % and 90 Hz for the first position. Also, the ANOVA results revealed that electrolyte concentration and machining voltage contributes around 62 % and 41 % respectively on the ECMM performance. Further, the quality of micro-hole on work material with the use of pulsed air supply to electrolyte was studied by obtaining scanning electron microscopy (SEM) images and checking the finish of the hole circumference.

1. INTRODUCTION

Monel 400 is a nickel-copper alloy with 67 % nickel 23 % copper content. Monel Alloy 400 possesses high strength, good malleability, fine electrical conductivity, and resistance against corrosion by acids and soluble gases. It is appropriate for applications where extreme temperature variations are encountered—from freezing point to as high as 1000°F (538°C), and it is solidified by means of cold-working. Since Monel 400 alloy exhibits good resistance against seawater salinity and high temperature steam, and impervious to stretch consumption breaking and pitting, it finds major

Int. J. Electrochem. Sci., 17 **(2022)** Article Number: 220846

2

applications in the marine field. Further it is also used for hydrocarbon handling, heat exchangers, and precision valves, electrical and electronic parts. Due to its good erosion resistance, it is readily used for compound handling, petrol refining pinnacles, clasps and fittings, siphons and valve parts and high-hazard applications as in the explosives industry and rocketry. Studies to understand the effect of using different electrolytes and applying mixing agents with electrolytes on the ECMM machining quality were carried out on various work materials. The effect of using passivating and non-passivating electrolytes on material removal rate (MRR), taper angle, and overcut were examined, and the optimal conditions of electrolyte and process combination to machine SMA were suggested for machining shape memory alloy (SMA) [1].

Experiments on A286 super alloy using separately plain $NaNO_3$ and ethylene glycol mixed $NaNO_3$ as electrolytes showed that good surface finish on the micro-hole circumference was achieved due to controlled power distributions in the mixed electrolyte case [2]. Also, mixing 20 % ethanol with ethylene glycol and sodium chloride electrolyte, to machine SMA, hampered the formation of oxide layers and hence improved machining quality [3]. By the influence of magnetic flux in citric acid solution applied by stationing rectangular bar magnets near the tool holder, for SS 304 work material, overcut was improved by 4.87 times due to effective removal of residual products from the machining zone [4]. Experiments using different electrolytes such as plain NaCl, NaNO3, and a combination of both, in equal weight-ratio, to machine nickel based alloy highlighted that lesser duty cycle and moderate frequency produced better micro-holes while using combined electrolyte [5]. The machining parameters for PH-Stainless Steel were studied by using different electrolytes such as NaCl, NaBr, $NaNO_3$, and a mixture of $NaNO_3$ and NaCl and the study inferred machining rate and radial over cut improved significantly with NaBr electrolyte while a better surface finish was obtained in the mixed NaNO3and NaCl electrolyte. Mixing of complex agent like Ethylenediaminetetraacetic acid (EDTA) is an aminopolycarboxylic acid, in the electrolyte hampered the oxide formation in work piece and resulted in good surface finish in the micro-holes as evidenced by the study on titanium alloy [6].

Employing different types of filters in the electrolyte to remove the polluted ions in ECMM process highlighted that the adsorbent improved the current flow in the electrolyte and hence enhanced the machining rate by 42 % as compared with normal recycling electrolyte [7]. Experiments using also Mixing of hydrogel with electrolyte in drilling micro-holes with high aspect ratio indicated that holes of 12 μm nominal diameter obtained with 50 % duty cycle, 5V machining voltage were 42 % better in surface finish than using normal electrolytes [8]. $NaNO_3$ electrolyte, with two different tools, namely plain graphite and liquid nitrogen treated graphite electrode, on SS 304, showed that the production of oxides on the work materials were absorbed by the electrodes resulting in good surface finish of micro-hole [9].

Applying pressurized electrolyte flow on SS 304 catalyzed the atomization of the electrolyte that led to improving machining speed by 52 %. Sending vibration using ultrashort pulse generator on Nithanol hindered the stay current of machining process and produced precise micro-holes [10]. The presence of magnetic field and ultraviolet rays for machining copper showed that such presence increased the machining rate and reduced the overcut significantly, due to the fast localization effect [11]. A 32 % rise in machining rate was recorded when ultrasonic vibration along with pressurized gas flow were directed onto the electrode, in the micro dimples fabrication process on SS 304, since the

current density in the electrolyte improved by about 7 % [12]. Experiments on using megasonic vibrations reported that machining rate was enhanced from 47 μm to 78 μm using the vibrations assisted electrolyte and the effect of localization was significantly prevented as confirmed by the micro pits formation [13]. When a layer of conductive absorption material was placed between the tool and the work piece, the unwanted flow of current in the electrolyte was prevented, resulting in better machining surface [14]. Heating the electrolyte using techniques like UV rays, ultrasonic vibration and hot air mixing method indicated that high heat energy increased the localization effect on the machining zone and produced high machining rate, and different forms of UV rays enhanced material removal and overcut in the work material [15-17].

Employing gas bubble chain on SS 304 work material with ethylene glycol electrolyte resulted in improved surface finish by two folds [18]. Optimizing the parameters using gray technique and experiments on ECMM with pulse generator on SS 304 indicated that 12V, 15 ms pulse on time, and 20 g/L electrolyte concentration, resulted in better machining rate [19]. Study on the effect of gas bubbles generated during machining revealed that the gas bubbles influenced the electrolyte temperature significantly and resulted in better machining rate and surface finish [20]. Application of inclined air shielding between the tool and electrode removed the electrolytic products continuously from the machining zone and enabled higher machining rate, and air velocity of 160 m/s and 8V machining voltage produced 2.5 times better machining rate compared with other electrolyte [21]. Supplying pulsated gas around the tool, to remove the machined debris, also formed gas films that acted as insulation and prevented undesired chemical reactions on the machining zone that improved the machining quality by 51 times better as compared with non-supply of pulsed gas [22].

The review of literature concerning the use of ECMM highlights that optimization of ECMM factors and employing suitable electrolytes play an important role in precision machining especially making micro-holes. Also, it is clear that, even though researches on ECMM using different electrolytes were studied, only a few researches have employed gas mixture with electrolyte and analyzed its effect such as experiments with ozonated electrolyte, hot air mixed electrolyte, oxygenated electrolyte, and gas bubbles mixture [23-25]. Among those methods, gas bubbles mixed electrolyte shows significant enhancement in machining performance. However, there is no study on employing pulsed gas supply, and optimization of ECMM factors and the electrolyte, for Monel 400 alloy. Further, since it is known that the application of gas supply to the electrolyte increases the conductivity of electrolyte and leads to higher dissolutions, its application for the machining of Monel 400 alloy using ECMM is an appropriate study.

Therefore, in this work, along with pulsed power supply to the system, atmospheric air is supplied through the tool holder. This novel attempt of supplying air to the tool is expected to enlarge the ions movement passage resulting in improved machining rate with lower overcut. Electrolyte concentration, machining voltage, duty cycle, and frequency are considered as the important machining parameters that are optimized using TOPSIS, VIKOR and COPRAS method. The output responses are assigned by entropy weight method. Furthermore, SEM image studies are done to understand the effects of pulsed air supply on the quality of micro-holes, by observing the finish of hole circumference. The paper is organized in the following sections: Section 2 describes the experimental details and parameter levels chosen for study. Section 3 gives the procedures for

weighting the responses, and for the multi-objective optimization techniques used. Section 4 contains outlines results and discussion, and Section 5 draws the conclusions of the study.

2. MATERIALS AND METHODS

2.1 Experimental arrangement

An indigenously developed experimental setup is used for conducting experiments. Figure 1a exhibits the photographic view and Figure 1b shows the tungsten tool electrode. The schematic arrangement of the setup is illustrated in Figure 1c.
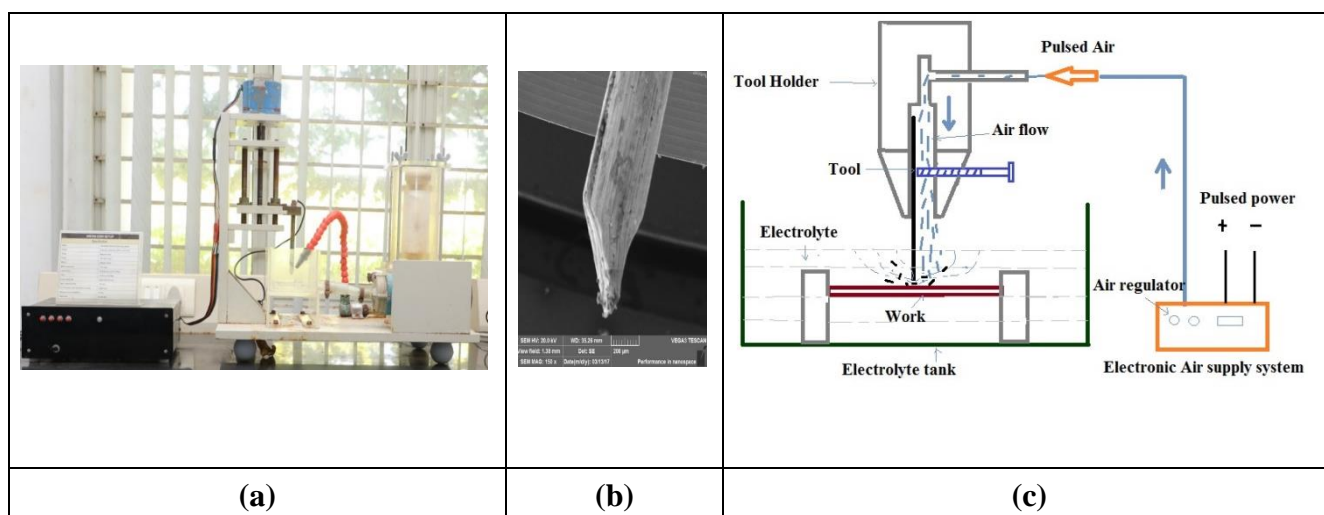

| **(a)** | **(b)** | **(c)** |

Figure 1. (a) ECMM experimental setup, **(b)** Tungsten tool electrode, and **(c)** Pulse air supply system

The setup comprises the electrolyte system with the electrolyte tank and the electrolyte, and work piece immersed in the electrolyte; electronic air supply system with pulse generator and air regulator; tool holding and feeding arrangement, and microcontroller. Monel 400 alloy of 0.8 mm thickness, is used as work piece and acts as anode. Tungsten electrodes of diameter 500 μm are used as cathode. The tool electrode is coated with epoxy resin to insulate it from stray current at the machining zone. Strong, non-toxic and highly conductive solid salt $NaNo_3$ is employed as electrolyte at different concentration levels.

2.2 L18 Orthogonal Array

The ECMM performance is evaluated using the MRR (Metal Removal Rate) and overcut evaluation with micro-holes. The micro-hole machining time is used to calculate MRR, and the differences between the diameters of tool electrode and the hole produced are considered for determining of overcut. Optical microscope is used to measure the micro-hole diameters. Micro-holes are identified by observing the presence of bubbles beneath the work plates. L18 Orthogonal Array (L18 OA) is planned including the most significant factors of ECMM namely machining voltage,

electrolyte concentration, duty cycle and frequency [15]. The levels of the machining factors and experimental planning are displayed in the Tables 1 and 2 respectively.

Table 1. Major influencing process factors and their ranges.

Symbol	Machining Factor	Level - I	Level - II	Level - III
C_e	Concentration of Electrolyte, g/L	24	26	28
V_m	Machining voltage, V	9	11	13
C_d	Duty Cycle, %	50	75	90
F	Frequency, Hz	70	80	90

Table 2. Experimental planning and responses

Ex. No.	C_e (g/L)	V_m (V)	C_d (%)	F (Hz)	MRR (µm / sec)	Overcut (µm)
1	24	9	50	70	0.528	160.96
2	24	11	75	80	0.7012	232.95
3	24	13	90	90	0.7012	224.57
4	26	9	75	80	0.3639	109.34
5	26	11	50	90	0.7806	135.76
6	26	13	90	70	0.8917	207.77
7	28	9	50	70	0.7806	129.75
8	28	11	90	80	0.7012	101.24
9	28	13	75	90	0.8917	124.95
10	24	9	90	90	0.5028	157.75
11	24	11	75	70	0.5106	209.76
12	24	13	50	80	0.6417	214.49
13	26	9	50	90	0.3917	128.30
14	26	11	90	70	0.6417	125.68
15	26	13	75	80	0.7806	191.37
16	28	9	90	80	0.7012	124.46
17	28	11	75	90	0.7806	153.24
18	28	13	50	70	0.2358	123.78

2.3 Optimization method

2.3.1 Entropy Weighting method

The Entropy weighting method is used for assigning weights to the output results of optimization methods. It consists of the following steps:

Int. J. Electrochem. Sci., 17 **(2022)** Article Number: 220846

6

Step 1. Write the output results in matrix form as indicated in Equation 1. It includes n characteristics and m alternatives for assessment.

$$\begin{bmatrix} k_{11} & k_{12} & k_{13} & ... & k_{1n} \\ k_{21} & k_{22} & k_{23} & ... & k_{2n} \\ \vdots & \vdots & \vdots & \vdots & \vdots \\ k_{m1} & k_{m2} & k_{m3} & ... & k_{mn} \end{bmatrix} \tag{1}$$

Step 2. Normalize or standardize output values using Equation 2.

$$M_{ij} = \frac{R_{ij}}{\sqrt{\Sigma_{i=1}^{m} V_{ij}^{2}}}, j = (1, 2, ..., n) \tag{2}$$

M_{ij} = a standardized range of value among the levels [0 to 1] for the ith and j^{th} quality.

Step 3. Calculate entropy value T_j using Equation 3.

$$T_j = -v\Sigma_{i=1}^{m} V_{ij} \ln(V_{ij}), j = (1, 2, ..., n) \tag{3}$$

Where, $v = 1/\ln(m)$ is invariable value and m is the number of choices.

Step 4. Calculate degree of deviation using Equation 4.

$$X_j = 1 - T_j \tag{4}$$

Step 5. Calculate the weight of output response using Equation 5.

$$R_{ij} = \frac{X_j}{\sqrt{\Sigma_{j=1}^{n} X_j}} \tag{5}$$

The familiar optimization methods of TOPSIS, VIKOR, and COPRAS are used to arrive at the optimal combination of the ECMM factors. All the three methods are used in order to check if the optimization results consistently indicate a particular optimal set of these factors.

2.3.2 TOPSIS Optimization Method

TOPSIS is an excellent tool to find out accurate optimal solutions based on limited experimental plans. The procedure to apply this method [16] is given below:

Step 1. Collect normalized output data from Equations 1 and 2 for decision matrix.

Step 2. The weight of each quality of responses is fixed as $Q_j (j = 1, 2, ..., n)$. The standardized weight for the decision matrix Q_{ij} is obtained from Equation 5.

Step3. The best and worst ideal results are calculated through Equations 6 and 7 respectively.

$$K^+ = \left\{ \Sigma_i^{\max} R_{ij} \,\middle|\, j \in J \right\}, \left\{ \Sigma_i^{\min} \,\middle|\, j \in J \,\middle|\, i = 1, 2, ..., m \right\}$$
$$= \left\{ x_1^+, x_2^+, x_3^+, ..., x_n^+ \right\} \tag{6}$$

$$K^- = \left\{ \Sigma_i^{\min} R_{ij} \,\middle|\, j \in J \right\}, \left\{ \Sigma_i^{\max} \,\middle|\, j \in J \,\middle|\, i = 1, 2, ..., m \right\} \tag{7}$$

$$= \left\{ x_1^-, x_2^-, x_3^-, ..., x_n^- \right\}$$

Step 4. The separations among the every positive option are estimated using Equation 8.

$$V_i^+ = \sqrt{\Sigma_{j=1}^n \left(Q_{ij} - x_j^+ \right)^2}, i = (1, 2, ..., m) \tag{8}$$

The separations among each negative option are estimated from Equation 9.

$$V_i^- = \sqrt{\Sigma_{j=1}^n \left(Q_{ij} - x_j^- \right)^2}, i = (1, 2, ..., m) \tag{9}$$

Step 5. The relations between the alternatives and ideal solutions are calculated using Equation 10.

$$B_i = \frac{i_i^-}{i_i^+ + i_i^-}, i = (1, 2, ..., m) \tag{10}$$

Step 6. The preference values B_i are graded in the descending order and ranked for finding the optimal combination of factors.

2.3.3. VIKOR Optimization Method

VIKOR is a multi-criteria optimization technique and it compromises solutions to classify the appropriate parameter result with the experiments. The procedure followed in this method [29] is given below:

Step 1. Obtain standardized values Equations 1 and 2. The output responses are allocated (-) value for minimization and (+) value for allocated for maximization.

Step 2. The highest $(a)_{\max}$ value and the least $(a)_{\min}$ value are taken from preference matrix for all results. Hence T_i and U_i values are intended by Equations 11 and 12.

$$C_i = \Sigma_{j=1}^n R_j \left[\left\{ (a_{ij})_{\max} - a_{ij} \right\} / \left\{ a_{\max} - a_{\min} \right\} \right] \tag{11}$$

$$D_i = \max^n of \left\{ \left[R_j(a)_{\max} - (a_{ij}) \right] / \left[(a)_{\max} - (a)_{\min} \right] \right\}, j = (1, 2, ..., n) \tag{12}$$

Where the weight of response is R_j evaluated according to the entropy weight method using Equations 1–5.

Step 3. The P_i values are estimated through the T_i and U_i values using Equation 13.

$$P = R \left\{ (C_i - C_{i-\min}) / (C_{i-\max} - C_{i-\min}) \right\} + (1 - R) \left\{ (D_i - D_{i-\min}) / (D_{i-\max} - D_{i-\min}) \right\} \tag{13}$$

Where $C_{i-\max}$ denotes the largest value of C_i and $C_{i-\min}$ denotes the smallest value of C_i. Similarly, $D_{i-\max}$ denotes the largest value of D_i and $D_{i-\min}$ denotes the smallest value of D_i. R -values are got from Equation 5.

Step 4. P_i, C_i and D_i values are ranked from smallest upwards. Based on the P_i value, the optimum result is obtained, and the minimum value of P_i whose rank is 1 is set as the most suitable value which is ranking as one.

2.3.4. COPRAS Optimization Method

COPRAS (Complex Proportional Assessment) method is an important technique to get the most positive results from the various options. This method lies in grading the preferred values obtained from the best and the worst outcomes. The measures ordered at the lower get the best combination of machining factor [13].

Step 1. Execute the regulated values from Equation 5 as in VIKOR technique.

Step 2. Distribute the weights to the regulated matrix using equation 14.

$$L_{ij} = E_{ij} \, X \, R_{ij} \tag{14}$$

Where, E_{ij} is the normalized values which are obtained from Equation 5. R_{ij} is weight assessment from Equation 8.

Step 3. Compute the largest and lowest option. Obtain the sum of weighted regulated value for the best and the worst choices using the Equations 15 and 16.

$$t_{i+} = \sum_{j=1}^{n} L_{+ij} \tag{15}$$

$$t_{i-} = \sum_{j=1}^{n} L_{-ij} \tag{16}$$

Where t_{i+} are the largest values and t_{i-} are the smallest values. Therefore, in this equation the largest value of t_{i+} is calculated as the best option and the smallest value of t_{i-} calculated as the next alternative.

Step 4. The priority values for the equivalent choices are arrived by means of equation 17.

$$W_i = t_{i+} + \sum_{i=1}^{m} t_{i-} \, / \, t_{i-} \sum_{i=1}^{m} \frac{1}{t_{i-}}, (i = 1, 2, ..., m) \tag{17}$$

The largest value of W_i is the best optimal solution.

Step 5. Evaluate the proportion of performance using Equation 18.

$$V_i = (W_i \, / \, W_{max}) x100 \tag{18}$$

Where, W_{max} is the largest relative extensive value.

3. RESULTS AND DISCUSSION

3.1 Effect of input variables on MRR

ECMM is performed on Monel 400 alloy and the effect of machining factors on MRR has been investigated. The relation between the machining factors chosen for the experiment and the MRR are plotted in Figure 2. The average values of MRR are chosen for plotting. From the plot, it is clear that, against the maximum value of each factor in its chosen range, the highest value of MRR is achieved. Further, the MRR increases almost at a constant rate with increasing values of each factor. The maximum and minimum MRR values are obtained at 13V machining voltage and 50 % duty cycle respectively. Additionally, the highest MRR of 0.59 µm/sec, achieved in this study by applying pulsated air in the electrolyte, is 42 % greater than the pure $NaNO_3$ electrolyte [12].
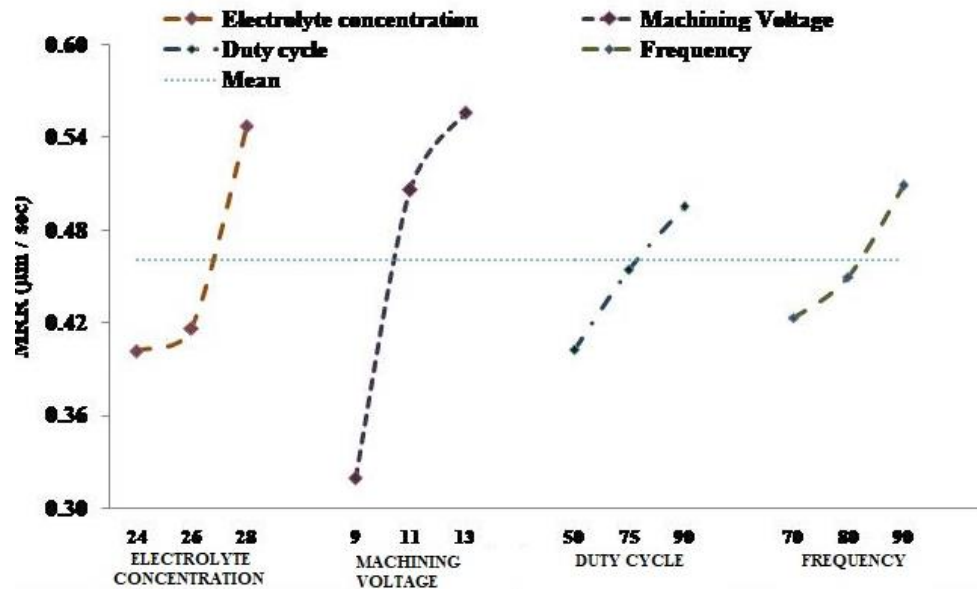
Figure 2. Effect of input variables on MRR

This experimental study confirms the fact that air supply in the electrolyte accelerates the atoms to act faster due to the viscosity changes. Further, the non-continuous pulsed air supply to the machining zone provides the passage for the electrochemical reactions that achieves higher MRR [26]. As observed from the plot, the subsequent lower MRRs are obtained by making changes in the electrolyte concentration and frequency. It is thus oblivious that an increase in electrolyte concentration increases the ions level in the electrolyte that leads to higher conductivity, and hence higher MRR. Also, increasing of parameter level stimulates the ion displacement in the electrolyte that results in higher MRR.

3.2 Effect of input variables on Overcut

Figure 3 represents the effect of input machining parameters on overcut by using pulsed air assisted electrolyte. The plot indicates that by increasing the electrolyte concentration, the overcut is increases.
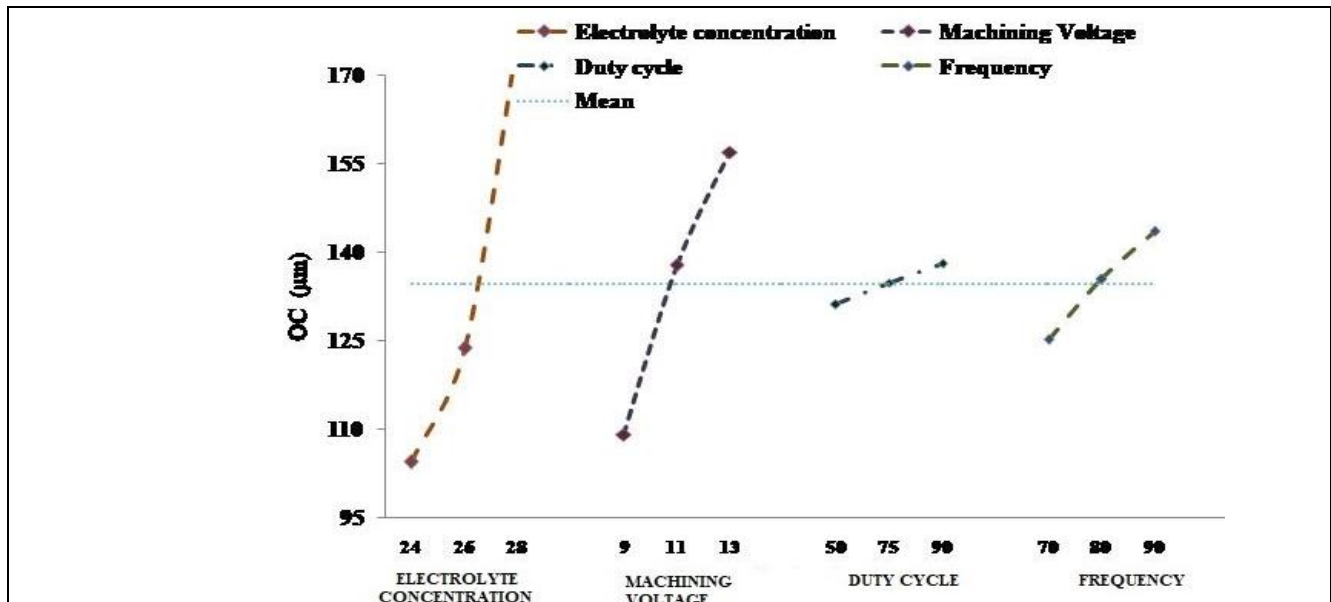
Figure 3. Effect of input variables on overcut

It is due to the fact that higher electrolyte concentration increases ion presence in the electrolyte, and hence improved conductivity. Along with this, atmospheric air supplied in electrolyte through tool holder removes dissolved products quickly from the inter electrode gap. Also, pulsed air provides an over gap for machining. Hence, the continuous material removal leads to excess machining and causes overcut [16].
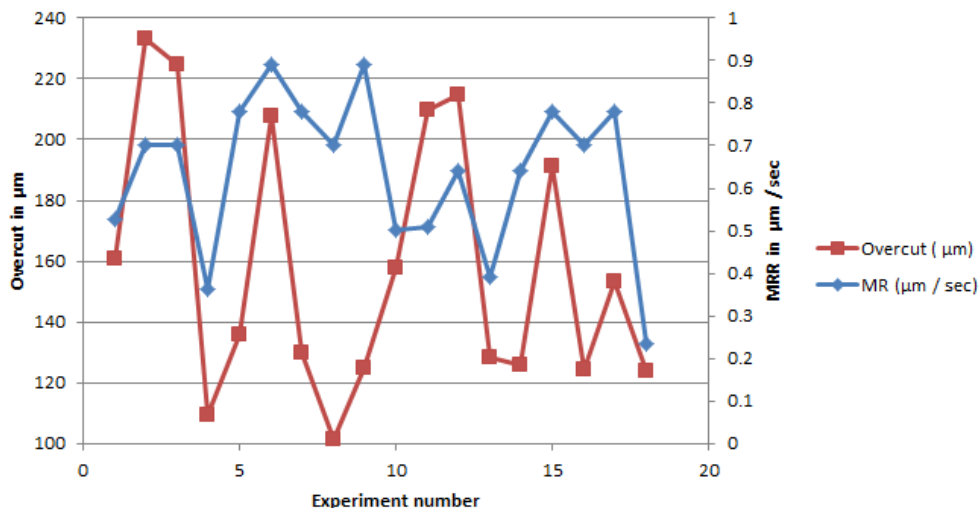

Figure 5. Relationship of ECMM parameter combination vis-à-vis Overcut, and MRR

The pulsed air triggers the repulsion displacement of electrolyte atoms which provides the excess energy for the electrolyte molecules and causes for the excess overcut [17]. The least and largest overcut are attained at 24 g/l and 28g/l electrolyte concentration levels respectively. Moreover,

higher values of machining parameters in the chosen range produce higher overcut. Hence, it is obvious that the addition of pulsed air provides additional energy to electrolyte molecules which causes the higher overcut.

The relationsip between the ECMM factor combinations (indicated by respective experiment number) on the abscissa, overcut (on the left side ordinate), and MRR (on the right side ordinate) are displayed in Figure 5.

3.3 Evaluation of best possible parameters combination

3.3.1. Calculation of weights for the output responses through entropy method

Table 3. Standardized values and weights for the outcomes

Ex. No.	Standardized outcomes		Ex. No.	Standardized outcomes		Ex. No.	Standardized outcomes	
	MRR	**Overcut**		**MRR**	**Overcut**		**MRR**	**Overcut**
1	0.187	0.231	7	0.277	0.186	13	0.139	0.184
2	0.249	0.335	8	0.249	0.145	14	0.228	0.180
3	0.249	0.322	9	0.316	0.179	15	0.277	0.275
4	0.129	0.157	10	0.178	0.227	16	0.249	0.179
5	0.277	0.195	11	0.181	0.301	17	0.277	0.220
6	0.316	0.298	12	0.228	0.308	18	0.084	0.178
Weights								
Responses				R_{ij}				
MRR				0.49				
Overcut				0.50				

The outcome of experimental results is exhibited in Table 3.These results are measured for the assessment of appropriate machining factor combination. The outcome values are standardized as homogeneous (unitless) values using Equations 4 and 5. These standardized values are used to calculate the weights for the MRR and overcut by applying the entropy method. The standardized values and the weights so obtained are presented in Table 3. The weights denote the relative importance among the machining parameters on ECMM performance. The overcut carries a slightly higher weight than MRR. These weights are used to scale the results obtained by the three optimization methods.

3.3.2. Evaluation of optimal combination using TOPSIS (B_i)

The suitable parameter combination for ECMM is calculated using TOPSIS method. The output responses such as MRR and overcut are assigned with weights that are estimated using the entropy method as presented in Table 3. The multi objective optimizations are converted into single objective optimization through combining of Taguchi and TOPSIS methods [15]. The largest B_i value is assigned rank one, the next highest value is given rank two, and so on. The ranking is presented in

Table No. 4. From the ranking of the B_i values, the parameter combinations used in 9th experiment, with B_i value of 0.8912, ranks first. Hence the combination, namely, 28 g/L of electrolyte concentration, 13V machining voltage, 75 % duty cycle, and 90 % Hz frequency is suggested by TOPSIS optimization to be the best optimal set of ECMM parameters. Experiment 7 and experiment 5, with B_i values of 0.8107 and 0.7899 respectively, rank second and third and they are the subsequently preferred optimal combinations.

Table 5. Optimal parameter combination ranking by TOPSIS optimization method

Ex No	V_{i+}	V_{i-}	B_i (Preference value)	Rank	Ex No	V_{i+}	V_{i-}	Bi (Preference value)	Rank
1	0.0774	0.0732	0.4861	11	10	0.0799	0.0718	0.4733	12
2	0.1006	0.0824	0.4502	15	11	0.1032	0.0514	0.3326	18
3	0.0949	0.0826	0.4653	14	12	0.0927	0.0731	0.4407	16
4	0.0936	0.0918	0.4951	10	13	0.0906	0.0802	0.4695	13
5	0.0317	0.1191	0.7899	3	14	0.0476	0.1054	0.6889	7
6	0.0766	0.1175	0.6052	8	15	0.0678	0.1009	0.5984	9
7	0.0284	0.1217	0.8107	2	16	0.0376	0.1135	0.7510	5
8	0.0337	0.1255	0.7883	4	17	0.0423	0.1122	0.7263	6
9	0.0171	0.1397	0.8912	1	18	0.1172	0.0785	0.4012	17

ANOVA test is done to understand the importance of each parameter in the machining quality. The TOPSIS preference values are studied numerically [16] and F-Test output is obtained to find the most important parameter for suitable machining performance.

Table 6. ANOVA for TOPSIS Preference values

Machining Factors	Degrees of freedom	SS	MS	F	Percentage of contribution
C_e	2	0.0835	0.0418	2.0393	17.38
V_m	2	0.0417	0.0209	1.0184	42.02
C_d	2	0.1410	0.0705	3.444	29.35
F	2	0.0123	0.0062	0.3009	2.56
Error	9	0.1843	0.0205		8.68
Total	**17**	**0.4628**	**0.0272**		**100**

Table 6, showing the result of ANOVA test, indicates that machining voltage plays the major role in machining with a 42.02 % contribution, while duty cycle contributes 29.35 %.

Table 7. Main effects for the TOPSIS Preference values

Machining factors	S/N ratio for TOPSIS			
	L - I	L - II	L- III	Delta
C_e	0.4414	0.6078	0.7281*	0.2868
V_m	0.5809	0.5670	0.6294*	0.0484
C_d	0.5883	0.6287*	0.5604	0.0404
F	0.5541	0.5873	0.6359*	0.0332
Optimal Parameter Combination by TOPSIS : 28 g/l, 13V, 75 % and 90 Hz				

Table 7 depicts the mean output results selected through Bi values. It mentions that machining voltage and duty cycle contributes a critical role in terms of machining performance. SS, MS, F, S/N mean Sum of Squares, Mean Square, F-test value, and sound to noise ratio respectively.

3.3.2. Evaluation of optimal combination using VIKOR (Pi)

The best optimal parameter combination for ECMM is estimated through VIKOR technique [15]. The output responses are assigned weights as in TOPSIS method for MRR and overcut. The values obtained from VIKOR technique are graded and least value is considered as first rank and the largest value as the last value as presented in Table 8. Thus, the least VIKOR value is chosen to indicate the optimal parameter solution. From the table, the combination in 9th experiment shows rank one. And hence is taken as the best optimal combination of parameters, that is, 28g/L electrolyte concentration, 13V machining voltage, 75 % duty cycle, and 90 Hz frequency. Combinations in experiments 8 and 7 are ranked as the other suitable combinations in that order.

Table 8. Optimal parameter combination ranking by VIKOR optimization method

Ex No	C_i	C_i	VIKOR (P_i)	Rank	Ex No	C_i	C_i	VIKOR (P_i)	Rank
1	0.5039	0.6178	0.7012	12	10	0.5108	0.6237	0.7119	13
2	0.6459	0.7355	0.9160	17	11	0.7027	0.7804	1.0000	18
3	0.6140	0.7098	0.8684	15	12	0.6210	0.7155	0.8788	16
4	0.4324	0.5548	0.5901	10	13	0.4834	0.6000	0.6696	11
5	0.2158	0.3405	0.2335	4	14	0.2832	0.4120	0.3485	7
6	0.4052	0.5300	0.5471	8	15	0.4273	0.5502	0.5821	9
7	**0.1930**	**0.3147**	**0.1932**	**3**	16	0.2333	0.3596	0.2637	5
8	**0.1449**	**0.2574**	**0.1059**	**2**	17	0.2823	0.4112	0.3471	6
9	**0.0902**	**0.1844**	**0.0000**	**1**	18	0.5848	0.6859	0.8244	14

Table 9. ANOVA for VIKOR values

Machining Factors	Degrees of freedom	SS	MS	F	Percentage of contribution
C_e	2	0.95165	0.47582	9.34	60.33
V_m	2	0.05112	0.02556	0.50	29.06
C_d	2	0.06346	0.03173	0.62	4.02
F	2	0.05266	0.02633	0.52	3.34
Error	9	0.45845	0.05094		3.24
Total	17	1.57735	0.09279		100

Table 10. Main effects of VIKOR values

Machining factors	S/N ratio for VIKOR			
	L - I	L - II	L- III	Delta
C_e	0.2891	0.4951	0.8460*	0.5570
V_m	0.5216	0.4918	0.6168*	0.0298
C_d	0.5367	0.6192*	0.4743	0.0625
F	0.4717	0.5561	0.6024*	0.0463
Optimal Parameter Combination by VIKOR : 28 g/l, 13V, 75 % and 90 Hz				

The influence of machining parameters on output results of MRR and overcut is studied statically through ANOVA method. The VIKOR values are chosen to determine the significant machining parameter and its contribution to the machining output. The contributions of each parameter over the output results are displayed in Table 9. According to the ANOVA results, the electrolyte concentration shows major contribution of 60.33 % on the ECMM performance. The next and least contributions are machining voltage (29.06 %) and frequency (3.34 %) respectively. The average VIKOR values are taken to obtain the main effects table that is displayed in Table 10, which is also associated with the optimal parameter combination.

3.3.3. Evaluation of optimal combination using COPRAS (q_i):

COPRAS technique is employed to determine the optimal parameter combination from L18 OA [27]. The result values are calculated using Equations 13—15, and displayed in Table 11. The percentage of each alternative corresponding to the input variables are estimated according to the q_i value from Equation 16 and the highest percentage is assigned rank one, and likewise, in the descending order.

Table 11. Optimal parameter combination ranking by VIKOR optimization method

Ex No	r_{i+}	r_{i-}	q_i	u_i (%)	Rank	Ex No	r_{i+}	r_{i-}	q_i	u_i (%)	Rank
1	0.0229	0.0282	0.0485	67.71	13	10	0.0218	0.0277	0.0480	66.91	15
2	0.0304	0.0409	0.0481	67.10	14	11	0.0221	0.0368	0.0418	58.33	18
3	0.0304	0.0394	0.0488	68.03	12	12	0.0278	0.0376	0.0470	65.64	16
4	0.0158	0.0192	0.0535	74.70	10	13	0.0170	0.0225	0.0492	68.59	11
5	0.0338	0.0238	0.0642	89.62	4	14	0.0278	0.0220	0.0607	84.63	7
6	0.0386	0.0364	0.0585	81.61	8	15	0.0338	0.0336	0.0554	77.28	9
7	**0.0338**	**0.0228**	**0.0656**	**91.58**	**3**	16	0.0304	0.0218	0.0636	88.67	5
8	**0.0304**	**0.0178**	**0.0712**	**99.30**	**2**	17	0.0338	0.0269	0.0608	84.77	6
9	**0.0386**	**0.0219**	**0.0717**	**100.00**	**1**	18	0.0102	0.0217	0.043586	60.81	17

Based on Table 11, combination of 9th experiment shows the highest percentage (100 %). Therefore, parameter combination of 9th experiment, that is, 28 g/l electrolyte concentration, 13V machining voltage, 75 % duty cycle and 90Hz frequency are taken as the best optimal parameter combinations. The experiments 8th and 7th follow as the subsequent suitable optimal combinations.

Table 12. ANOVA table for COPRAS values

Machining Factors	Degrees of freedom	SS	MS	F	Percentage of contribution
C_e	2	0.00076	0.00038	6.56	51.60
V_m	2	0.00005	0.00002	0.40	35.37
C_d	2	0.00009	0.00005	0.79	6.18
F	2	0.00005	0.00003	0.48	3.74
Error	9	0.00052	0.00006		3.12
Total	17	0.00146	0.00009		100

Table 13. Main effects of COPRAS values

Machining factors	S/N ratio for COPRAS			
	Level - I	Level - II	Level- III	Delta
C_e	0.0470	0.0569	0.0627*	0.0157
V_m	0.0547	0.0542	0.0578*	0.0031
C_d	0.0553	0.0584*	0.0530	0.0031
F	0.0531	0.0565	0.0571*	0.0033
Optimal Parametric Combination by COPRAS: 28 g/L, 13V, 75 % and 90 Hz.				

ANOVA results for COPRAS values are presented in Table 12, and main effects of the ANOVA results are shown in Table 13. Electrolyte concentration contributes 51.60 % for machining performance, and machining voltage contributes around 35.37 %. Frequency has the least effect with a contribution of only 3.74 %. Therefore, based on the table electrolyte concentration impacts more on the machining performance compare to Ether parameters. The optimal process parameters are correlated in the main effects table with the parameter levels, i.e., 28 g/l, 13V, 75 % and 90 Hz.

3.3.4 Quality of micro-hole machined

The SEM images of micro-holes are displayed in Figures 6 (a) and (b) for the first two optimal combinations of all the three optimization techniques. such as TOPSIS, VIKOR and COPRAS method. The image for the best optimal combination of parameters indicates micro-hole with a very good finish on the rim of the hole circumference. The image for second combination illustrates micro hole with minute pits on the machined area. Figure 6 (c) depicts the optical microscopy images of the micro-hole.
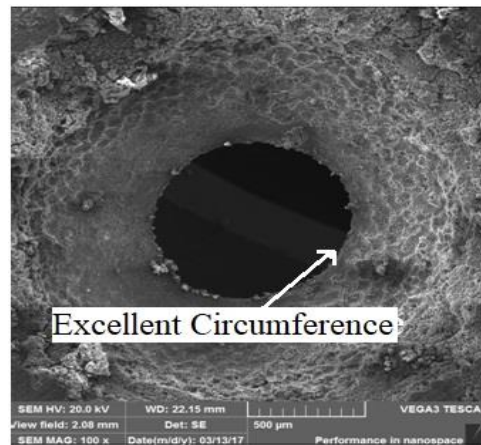

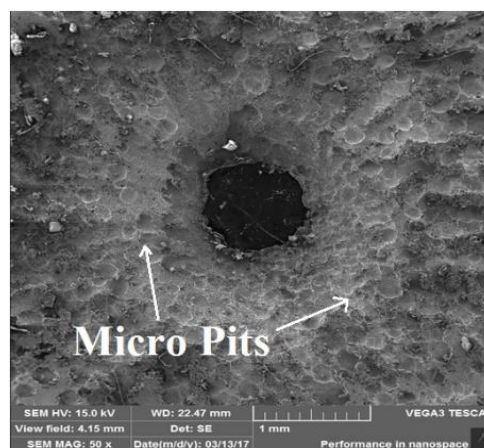**Figure 4 (a).** SEM image showing micro hole machined with best optimal combination (9th experiment).

Figure 4 (b). SEM image showing micro hole generated with 2nd Optimal combination (7th experiment).
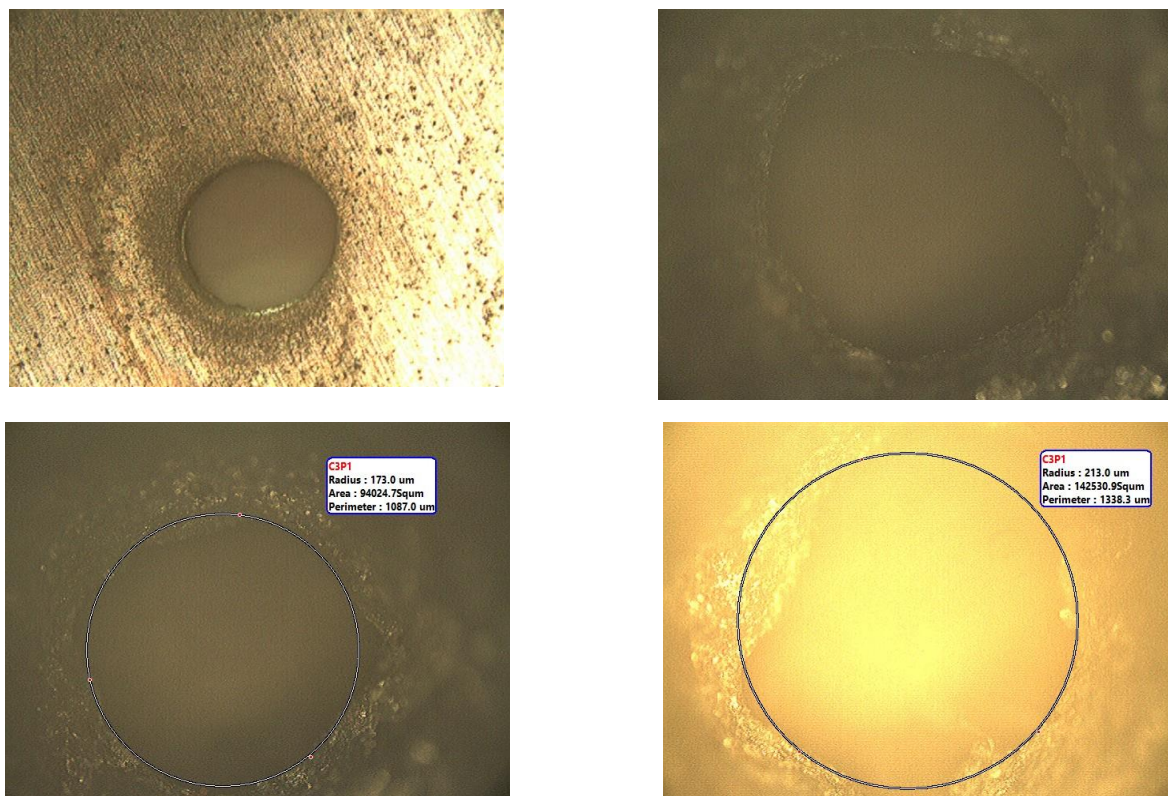
Figure 4 (c). Optical microscopy images of micro hole.

4. CONCLUSION

The primary objective of this work is to study the effect of supplying pulsed atmospheric air on the performance of ECMM on Monel 400 alloy, by framing L18 orthogonal array. The pulsed air is supplied between the tool and electrolyte through the tool holder. Optimization techniques such as TOPSIS, VIKOR and COPRAS are used to determine the best optimal combination of the machining parameters.

The study reveals that MRR increases almost constantly with increasing values of the parameter levels. The largest MRR of 0.59 µm/sec, obtained in this study with the application of pulsed air supply at the electrode, is 42 % higher than using only $NaNO_3$ electrode. This result clearly confirms that using pulsed air supply is advantageous in achieving higher MRR. The ANOVA results clarify that electrolyte concentration and machining voltage contributes majorly for the ECMM quality. The results of optimization, done through the TOPSIS, VIKOR, and COPRAS methods, consistently indicate the same machining parameter combination as the best optimal combination. Further, it is visually observed that the same optimal combination produces micro-holes with good quality as evidenced by the finish of the hole circumference. However, the heat energy of the electrolyte also produces small micro fractures on the surface nearby the micro-holes.

References

1. Mouliprasanth, P. Hariharan, *Russ. J. Electrochem*, 57(3) (2021) 197.
2. E. Rajkeerthi, P. Hariharan, *Surf. Topogr. Metrol. Prop*, 9 (4) (2021) 045033.
3. S. Ao, K. Li, W. Liu, X. Qin, T. Wang, Y. Dai and Z. Luo, *J. Manuf. Processes*, 53 (2020) 223.
4. J.R. Vinod Kumaar and R. Thanigaivela,. *Mater. Manuf. Processes*, 35(9) (2020) 969.
5. S. Kunar, E. Rajkeerthi, K. Mandal and B.Bhattacharyya, *Manuf. Rev*, 7 (2020) 15.
6. Thakur, M. Tak and R.G. Mote, *Procedia Manuf*, 34 (2019) 355.
7. S. Önel, G. Ergin, *J. Manuf. Sci. Eng*, 142(7) (2020) 074502.
8. H. Zhang, S.Ao, W. Liu, Z. Luo and K.Guo, *Int. J. Adv. Manuf. Technol*, 91(9) (2017) 2965.
9. P. Natarajan, S.S. Karibeeran and P.K. Murugesan,.. *J. Braz. Soc. Mech. Sci. Eng.,* 43(11) (2021) 1.
10. J.C. Hung, P.J. Yang, *Processes*, 9(10) (2021) 1752.
11. K.G. Saravanan, T. Rajasekaran and M. Soundarrajan, *Bull. Pol. Acad. Sci. Tech. Sci*, (2021) 138816.
12. M. Wang, X. Chen, W. Tong, J. Wang, and X. Wang, *Int. J. Adv. Manuf. Technol*, 107(1) (2020) 157.
13. K. Zhai, L. Du, Y. Wen, S. Wang, Q. Cao, X. Zhang and J. Liu, *Ultrason*, 100 (2020) 105990.
14. W. Natsu, J. He, and Y. Iwanaga, *Procedia CIRP*, 87 (2020) 263.
15. M. Soundarrajan, R. Thanigaivelan, *Russ. J. Appl. Chem*, 91(11) (2018) 1805.
16. M. Soundarrajan, R. Thanigaivelan, *Lec Nots on Multi Ind. Eng. (2019) Springer, Singapore.*
17. M. Soundarrajan, R. Thanigaivelan, *Russ. J. Electrochem*, 57(2) (2021) 172.
18. N. Qu, C. Gao, *J. Mater. Process. Technol*, 294 (2021) 117136.
19. V. Subburam, S. Ramesh and L.I. Freitas, *Fut Trends Intell. Manuf*. 33 (2021). *Springer, Cham*.
20. M.H.Wang, W.J. Tong, G.Z. Qiu, X.F. Xu and J. Mitchell-Smith, *J. Manuf. Processes*, 43 (2019) 124.
21. Y. Pan, Z. Hou and N. Qu, *Int. J. Adv. Manuf. Technol*, 100(5) (2019) 1767.
22. S. Zhan, Y. Zhao, *J. Mater. Process. Technol*., 291 (2021)
23. X. Chen, N. Qu, X. Fang and D. Zhu, *Surf. Coat. Technol*., 277 (2015) 44.
24. H.D.He, N.S. Qu, Y.B. Zeng and P.Z. Tong, *J. Electrochem. Soc*, 164(9) (2017) E248.
25. M. Soundarrajan, R. Thanigaivelan, S. Maniraj, *Int Adv in Ind. Autom and Smart Manuf. (367) (2021) Springer, Singapore.*
26. M. Soundarrajan, R. Thanigaivelan, S. Maniraj, *In Adv in Ind. Autom and Smart Manuf. (367) (2021) Springer, Singapore.*
27. Petkovic, Dusan, Madić, Miloš and G. Radenkovic, *Sci. Sintering*. 47 (2015) 229.
28. https://www.specialmetals.com/documents/technical-bulletins/monel-alloy-400.pdf